High glucose induces podocyte epithelial-to-mesenchymal transition by demethylation-mediated enhancement of MMP9 expression

LI LING, LIBO CHEN, CHANGNING ZHANG, SHUYAN GUI, HAIYAN ZHAO and ZHENGZHANG LI

Department of Endocrinology, Guangdong Medical College Affiliated Shenzhen Nanshan Hospital,
Shenzhen, Guangdong 518052, P.R. China

Abstract. Abnormal expression of matrix metalloproteinase 9 (MMP9) is correlated with podocyte epithelial-to-mesenchymal transition (EMT) in diabetic nephropathy (DN). However, the mechanisms underlying this process are not well defined. Site-specific demethylation may sustain high expression levels of target genes. In the present study, in order to investigate the association between DNA demethylation of MMP9 promoter and podocyte EMT in DN, human podocytes were cultured in high-glucose (HG) medium and a rat model of DN was established by intraperitoneal injection of streptozotocin (STZ) to determine whether site-specific demethylation of the MMP9 promoter was involved in regulating podocyte EMT in DN. The MTT assay was used to assess the effects of HG culture on the growth of podocytes, and the demethylation status of the MMP9 promoter was assessed by bisulfite sequencing polymerase chain reaction. mRNA and protein expression levels of MMP9, α-smooth muscle actin (α-SMA), podocalyxin and fibronectin-1 in podocytes were assessed by reverse transcription-quantitative PCR (RT-qPCR) and western blot analyses. The results demonstrated that HG treatment up regulated the expression of MMP9, α-SMA and fibronectin-1, but down regulated the expression of podocalyxin in podocytes. The MMP9 promoter region was revealed to contain a variety of demethylated CpG sites, and HG treatment reduced the rate of MMP9 promotermethylation, which, in turn, enhanced its promoter activity. In summary, these data suggested that demethylation of the MMP9 promoter may serve an important role in podocyte EMT in DN. The demethylation status of the MMP9 promoter maybe used as an important prognostic marker of DN in clinic.

Correspondence to: Dr Libo Chen, Department of Endocrinology, Guangdong Medical College Affiliated Shenzhen Nanshan Hospital, 89 Taoyuan Road, Nanshan, Shenzhen, Guangdong 518052, P.R. China
E-mail: chenlibo_1979@126.com

Introduction

Diabetes-induced kidney disease is a common complication in patients with diabetes, and may lead to end-stage renal failure (1-3). Diabetic nephropathy (DN) is the most severe complication of diabetes and is also a major contributor to end-stage renal failure (4). Podocytes are highly specific cells that are located at the outer surface of the glomerular basement membrane; they aid in maintaining the structure and function of the glomerular filtration barrier (5). Podocyte damage may lead to kidney dysfunctions such as diabetic proteinuria (6,7). Damage and loss of podocytes is observed in patients with diabetes and may represent an early phase of DN, and the loss of podocytes is considered to be a key factor that causes DN (8-10).

The abnormal expression of fibroblast-specific protein in renal tubular epithelial cells was suggested to indicate that some myofibroblasts may have been derived from the transformation of epithelial cells (11). A previous study reported that, during renal fibrosis, a large portion of tubular epithelial cells may undergo epithelial-to-mesenchymal transition (EMT) to become myofibroblasts (12). However, the specific mechanisms involved in podocyte EMT in DN remain to be characterized.

During the early phase of DN, podocyte EMT may be promoted by a number of factors, such as matrix metalloproteinases (MMPs). Diabetes has been associated with the abnormal expression of MMP proteins, particularly MMP9 (13). The expression of MMP9 may be induced by exposure to external stimuli such as reactive oxygen species (ROS). Generation of excessive ROS levels in podocytes may activate the extracellular

signal-regulated kinase 1/2 signaling pathway and ultimately induce the expression of MMP9 (14); therefore, increased ROS levels may cause podocyte injury. *S*-nitrosylation of certain proteins in the cell is a marker of oxidative stress, and during the onset of diabetes, protein *S*-nitrosylationis enhanced (15). *S*-nitrosylation was reported previously to activate the expression of MMP9 and to induce apoptosis of neuronal cells. One of the main components of the glomerular basement membrane (GBM) is type IV collagen (16), and over expression of MMP9 may alter the composition of the GBM, which may result in structural changes inpodocytes and their eventual loss from the GBM (17). MMP9 may suppress the expression of podocalyxin inpodocytes, reducing the charge barrier that prevents microalbuminuria. High-glucose (HG) levels or transforming growth factor (TGF)-β treatment were reported to induce the expression of MMP9 proteins in podocytes (18). MMP9 expression has been associated with the activation of integrin-linked protein kinase, which promotes the adhesion of podocytes to the GBM (19). Notably, it was previously reported that the level of podocytes in the urine of patients with chronic kidney disease was closely associated with the plasma expression level of MMP9, and MMP9 polymorphisms may influence the incidence rate of DN (20). These data suggested that MMP9 may serve a key role in podocyte injury and glomerulopathy.

The methylation and demethylation of genes is a form of epigenetic modification that has been implicated in a number of biological processes (21). Site-specific demethylation is able to dynamically regulate gene expression, which allows cells to adapt to external stimuli (22). Previous studies indicated that alterations in the DNA methylation status in mouse thymic lymphoma cell lines were able to affect the transcriptional activity of the MMP9 promoter, and thereby affect the expression of MMP9 (23,24). Demethylation of certain CpG sites in the MMP9 promoter was reported to disrupt the synthesis of MMP9 in cartilage tissues during osteoarthritis (25). The aim of the present study was to assess whether demethylation of the MMP9 promoter region may bea key regulatory factor in determining podocyte EMT in DN, and to investigate whether MMP9 promoter demethylation may represent a prognostic marker of DN.

Materials and methods

Cell culture. Human renal epithelial tissues were obtained from the unaffected pole of tumor-bearing kidneys of adults; kindly supplied by Department of Urology, Zhujiang Hospital, Southern Medical University (Guangzhou, China), and human podocytes were isolated from renal epithelial tissue and developed by transfection with the temperature-sensitive SV40-T gene by Guangzhou Scirince (Scirince, Guangzhou, China) (26). Podocytes were maintained at 37˚C in a humidified atmosphere of 95% air and 5% CO_2. Cells were cultured in RPMI-1640 medium (Sigma-Aldrich; Merck KGaA, Darmstadt, Germany) supplemented with 10% fetal bovine serum, 100 U/ml penicillin and 100 mg/ml streptomycin (Sigma-Aldrich; Merck KGaA). The cell culture medium was changed once every 2 days.

Cell transfections. Podocytes were cultured for 2 weeks at 37˚C to induce cell differentiation, after which $1x10^6$ podocytes/ml were transferred to a 6-well cell culture plate and transfected with predesigned MMP9-directed small interfering (si)RNA (sense 5'-GACCUGGGCAGA UUCCAA Att-3', antisense 5'-UUUGGA AUCUGCCCA GGUCtg-3'; Guangzhou Ribo Bio Co., Ltd., Guangzhou, China) using Lipofectamine® 2000 (Invitrogen; Thermo Fisher Scientific, Inc., Waltham, MA, USA) with 50 nM transfection concentration at room temperature. Scramble siRNA was used as a control. Cells were transfected for 24 h at room temperature, after which the culture medium (RPMI-1640 medium supplemented with 10% fetal bovine serum, 100 U/ml penicillin and 100 mg/ml streptomycin) was replaced with RPMI-1640 culture medium containing 10% FBS, 1% insulin-transferr in-sodium selenite (ITS) and either 5.0 mmol/ld-glucose [normal glucose (NG) group] or 25 mmol/l d-glucose [high glucose (HG) group], and cells were cultured for an additional 24 h prior to further evaluation at 37˚C. Experiments were performed in triplicate. RPMI-1640 media, FBS and ITS were all purchased from Sigma-Aldrich (Merck KGaA).

Immunofluorescence assay. Podocytes were fixed with ice-cold 4% paraformaldehyde for 15 min and blocked with 5% goat serum (Sigma-Aldrich; Merck KGaA) with 0.3% Triton X-100 for 15 min at room temperature, then incubated with MMP9 primary antibody (1:200, ab38898; Abcam, Cambridge MA, USA) overnight at 4˚C. The cells were subsequently washed 3 times with 0.1 mol/l PBS, followed by incubation with fluorescein isothiocyanate (FITC)-conjugated secondary antibody (1:600, ab150117; Abcam) for 1 h at 37˚C. Experiments were performed in triplicate. Images were captured using an Olympus BX51 fluorescence microscope (Olympus Corporation, Tokyo, Japan).

Flow-cytometric analysis. Following siRNA transfection and induction cells were cultured for 24 h at 37˚C. The cells were collected for 5 min at 300 x g at 4˚C, washed twice and re suspended with PBS at $1x10^6$ cells/ml. Cells were stained with FITC (5 μg/ml) and propidium iodide (5 μg/ml) for 15 min at room temperature (20-25˚C) in the dark, and the fraction of living, dead, early apoptotic and late apoptotic cells was assessed by BD FACS Aria II flow cytometer (BD Biosciences, Franklin Lakes, NY, USA). The Annexin V-FITC Apoptosis Detection kit was purchased from Abcam (ab14085). Experiments were performed in triplicate.

MTT assay. To analyze the effects of HG culture on podocyte activity, we assessed cell proliferation using the Cell Proliferation Reagent kit I (Sigma-Aldrich; Merck KGaA). Podocytes were seeded ($5x10^4$ cells/well) in a 96-well plate and cultured at 37˚C for 24 h. The different concentrations of glucose were added to the media, and the plate was incubated at 37˚C for 0, 24, 48, 72 and 96 h, after which cells were transferred to fresh medium [RPMI-1640 medium (Sigma-Aldrich; Merck KGaA) supplemented with 10% fetal bovine serum, 100 U/ml penicillin and 100 mg/ml streptomycin (Sigma-Aldrich; Merck KGaA)] containing 1 mg/ml MTT (Invitrogen; Thermo Fisher Scientific, Inc.) and cultured for 3 h at 37˚C. The medium was removed, dimethylsulfoxide (100 μl) was added and the plate was agitated for 20 min

at room temperature to completely dissolve the purple formazancrystals, and absorbance was measured at 570 nm. Experiments were performed in triplicate.

Reverse transcription-quantitative polymerase chain reaction (RT-qPCR). Total RNA was isolated from human podocytes using TRIzol reagent (Invitrogen; Thermo Fisher Scientific, Inc.) and reverse transcribed Prime Script TMRT reagent kit (Takara Bio, Inc., Otsu, Japan) according to the manufacturer's instructions. qPCR was performed using SYBR Premix ExTaq (Takara Bio, Inc.) and an ABI7500 Real-Time PCR instrument (Applied Bio systems; Thermo Fisher Scientific, Inc.) with the following cycling conditions: 95°C for 10 min, followed by 40 cycles of denaturation at 95°C for 10 sec, annealing at 60°C for 10 sec and extension at 72°C for 20 sec. The primer sequences used for qPCR are provided in Table I. RT-qPCR results were analyzed using ABI7500 system software (7500 v2.3, Applied Bio systems; Thermo Fisher Scientific, Inc.). The $2^{-\Delta\Delta Cq}$ method was used to detect the relative expression of Mrna (27), the GAPDH was used to normalize the mRNA expression levels and the relative quantification cycle (Cq) values were reported as expression fold alterations. Experiments were performed in triplicate, the data averaged.

Western blot analysis. The transfected podocytes were washed twice with ice-cold PBS solution, and lysed inlysis buffer (Sigma-Aldrich; Merck KGaA). Total protein was quantified with Bicinchoninic Acid Protein Assay kit (Beyotime Institute of Biotechnology, Haimen, China) according to the manufacturer's protocols, and 50 μg/well protein was used for SDS-PAGE (10%) electrophoresis and transferred to a polyvinylidene fluoridemembrane and then the membrane was blocked for 1 h at room temperature. Blocking Reagent was purchased from Beyotime Institute of Biotechnology. The membranes were incubated overnight with primary antibodies directed against MMP9 (1:500, sc-21736), α-smooth muscle actin (α-SMA, 1:500, sc-71625), podocalyxin (1:500, sc-23904), fibronectin-1 (1:500, sc-69681) and GAPDH (1:500, sc-293335) at 4°C; all purchased from Santa Cruz Biotechnology, Inc. (Dallas, TX, USA). Subsequently, the membranes were incubated for 2 h with horseradish peroxidase (HRP)-conjugated secondary antibody (bovine anti-mouse 1:200, sc-2371, Santa Cruz Biotechnology, Inc.) at room temperature, and protein bands were visualized using the Super Signal Chemiluminescent Substrate (Pierce; Thermo Fisher Scientific, Inc.). Experiments were performed in triplicate. Protein expression of MMP9, α-SMA, podocalyxin and fibronectin-1 were normalized to GAPDH. The blots were analyzed using Quantity One software, version 4.6 (Bio-Rad Laboratories, Inc., Hercules, CA, USA).

DNA demethylation analysis. Cells ($1x10^6$) in the NG and HG groups were collected, washed with PBS twice, and genomic DNA was extracted from cells using the QIAamp DNA Mini kit (Qiagen, Inc., Valencia, CA USA), according to the manufacturer's instructions. Following hydrosulphite treatment of DNA using the EpiTect Bisulfite kit (Qiagen, Inc.) according to the manufacturer's protocols, the demethylation status of the MMP9 promoter was assessed by hydrosulphite sequencing PCR using ABI7500 Real-Time PCR instrument

Table I. Primer sequences used in reverse transcription-quantitative polymerase chain reaction.

Gene	Primer sequence (5'→3')
MMP9	F: GGGACGCAGACATCGTCATC
	R: TCGTCATCGTCGAAATGGGC
α-SMA	F: GTGTTGCCCCTGAAGAGCAT
	R: GCTGGGACATTGAAAGTCTCA
Podocalyxin	F: AGCTAAACCTAACACCACAAGC
	R: TGAGGGGTCGTCAGATGTTCT
Fibronectin-1	F: CGGTGGCTGTCAGTCAAAG
	R: AAACCTCGGCTTCCTCCATAA
GAPDH	F: CCTTCATTGACCTCAACTACAT
	R: CCAAAGTTGTCATGGATGACC

α-SMA, α-smooth muscle actin; F, forward; R, reverse; MMP9, matrix metalloproteinase 9.

(Applied Bio systems; Thermo Fisher Scientific, Inc.) with the following clones made under the cycling conditions: 95°C for 10 min, followed by 40 cycles of denaturation at 95°C for 1 min, annealing at 60°C for 1 min and extension at 60°C for 10 min, and promoter-specific primers: MMP9 forward 5'-GATGGG GGATTTTTTTAGTTTTATT-3' and reverse 5'-TACCCACCT CTACCAACTACCTATC-3'. Ten clones of each DNA sample were selected via gel extraction for verification.

Dual-luciferase reporter assays. The effects of CpG-site methylation on MMP9 promoter activity were examined *in vitro* using the pGL3-Basic vector (Promega Corporation, Madison, WI, USA). PCR primers were designed with *Not*I and *Xho*I restriction cut sites in the 5' ends; MMP9 promoter forward 5'-cgcgcggccgcAGAGGAAGCTGAGTCAAAGAAG GC-3' and reverse 5'-cccctcgagTGGTGAGGGCAGAGGTGT CT-3'. PCR cycling conditions: 95°C for 10 min, followed by 40 cycles of denaturation at 95°C for 10 sec, annealing at 60°C for 30 sec and extension at 72°C for 20 sec, 1 cycle at 72°C for 7 min; and a final hold at 4°C. The primers were used to amplify a 260 bp DNA fragment from the human MMP9 promoter region. The obtained DNA fragments were ligated into the multiple cloning sites of the pGL3-Basicvector. pGL3-MMP9 plasmids were recovered and plasmid methylation was performed using EpiXplore™ Methylated DNA Enrichment kit (Takara Bio, Inc.), according to the manufacturer's instructions. Following methylation, the plasmids (0.02 μg/μl) were transformed into 293T (American Type Culture Collection, Manassas, VA, USA) cells (10^5 cells/well) using Lipofectamine® 2000 (Invitrogen; Thermo Fisher Scientific, Inc.) in 96-wellplate. Cells were cultured for 24 h at 37°C, luciferase activity was assessed by using QUANTI-Luc reagent (Invivogen, San Diego, CA, USA) and a PerkinElmer EnVision 2104 Multi label Plate Reader (PerkinElmer, Inc., Waltham, MA, USA), according to the manufacturer's protocols. All experiments were repeated three times.

Animals and treatments. Male adult Wistar rats (180±16 g) were purchased from the Guangdong Medical Laboratory

Animal Center [Guangzhou, China; Animal license number SYXK (Guangdong): 20130002]. Rats were acclimated for 7 days at room temperature under normal lighting conditions. All animal experiments were approved by the Animal Research Ethics Board of Sun Yat-sen University (Guangzhou, China) and were carried out in compliance with institutional guidelines on the care of experimental animals. All efforts were made to minimize the suffering of animals; experiments with animals were conducted in Sun Yat-sen university laboratories due to equipment availability and access. In the DN model group, diabetes was induced by intravenous injection of streptozotocin (STZ; 65 mg/kg; Sigma-Aldrich; Merck KGaA), where as normal Control rats received citric acid (100 mmol/l) administered by intravenous injection (28). The blood glucose levels were measured every day from tail vein blood using a Bayer Contour glucose meter (Bayer, Pittsburgh, PA, USA), if the blood glucose level was >16.7 mmol/l for >10 days, the rats were defined as a successful DN model. At week 2 and week 6, rats were photographed, the blood glucose levels and body weight were recorded. At week 6 rats were sacrificed and kidney tissues were collected.

Kidney flush, glomeruli isolation, podocyte isolation and subculture. Saline was injected into the distal artery of the renal artery to wash blood from the tissue. Glomeruli were separated as described previously (29). Briefly, kidney tissue was cut into pieces, which were digested with collagenase IV (200 U/ml, Sigma-Aldrich, Merck KGaA) for 1 h under constant rotation at 37°C, and passed through a 100-mesh sieve (150 μm). The resulting cell suspension was sieved using a 200-mesh sieve (75 μm), and the glomeruli were retained on the sieve surface. The podocyte from isolation was used for DNA demethylation assay and western blot analysis. The protocol of demethylation analysis here was conducted as aforementioned.

Immunohistochemistry. The kidney tissues collected from rats were embedded in paraffin and sectioned (4 μm). Paraffin-embedded tissues sections were deparaffinized with xylene and rehydrated and fixed with 2% paraformaldehyde, 4% sucrose in PBS for 10 min at room temperature and then permeabilized with 0.3% Triton X-100 (Sigma-Aldrich, Merck KGaA) in PBS for 10 min. Sections were washed 3 times in PBS, and incubated for 30 min at room temperature in 3% bovine serum albumin (Gibco; Thermo Fisher Scientific, Inc.) in PBS to prevent nonspecific binding. The sections were subsequently incubated with primary antibodies against MMP9, α-SMA, podocalyxin, fibronectin-1overnight at 4°C in a moist chamber, then HRP-labeled secondary antibody as aforementioned for 2 h at room temperature. 3,3'-diaminobenzidine (Sigma-Aldrich; Merck KGaA) was added for 2 h at room temperature, and the sections were counterstained using hematoxylin for 5 min at room temperature, then air dried, and images were captured using a Leica DM5000B microscope equipped with a Leica DFC500 camera and Image Pro Plus software (vs 5.02; Media Cybernetics, Inc., Rockville, MD, USA). Five randomly chosen high-power fields (100 cells/visual field) were visualized. The percentage of positively staining cells were counted manually and analyzed using Image J software v1.48 (National Institutes of Health, Bethesda, MD, USA). The staining intensity of MMP9, α-SMA, podocalyxin and fibronectin-1 were normalized to MMP9 control.

Statistical analysis. Statistical analysis was performed using SPSS 19.0 (IBM Corp., Armonk, NY, USA) and Graph Pad Prism 5 (Graph Pad Software, Inc., La Jolla, CA, USA) software. Data are presented as the mean ± standard error of the mean, determined using single factor analysis of the variance (ANOVA). Statistical significance was evaluated by one-way ANOVA followed by least significant difference test or Dunnett's T3 post hoc analysis. $P<0.05$ was considered to indicate a statistically significant difference.

Results

HG-treatment inducespodocyte apoptosis and suppresses proliferation in vitro. To determine the relationship between MMP9 expression pattern and glucose treatment in podocyte EMT in DN, MMP9 gene silencing was performed with siRNA in podocyte cultures. Immunofluorescence assay results demonstrated that the expression of MMP9 in cells transfected with MMP9-siRNA was lower than the untransfected control cells (Fig. 1A). Results of western blot analysis confirmed that the expression of MMP9 protein in podocytes transfected with MMP9-siRNA was significantly lower compared with the Control group (Fig. 1B; $P<0.05$). Following incubations with glucose, the rate of podocytes apoptosis was assessed by flow cytometry. The data revealed that apoptotic rates were significantly higher following incubation with high concentrations of glucose compared with incubation with normal physiological concentrations of glucose. Following high glucose treatment, the rate of (early) apoptosis was also significantly higher in podocytes without siRNA than with MMP9 siRNA treatment (Fig. 1C and D; $P<0.05$). Results from the MTT assay indicated that incubation in a high concentration of glucose significantly reduced human podocyte proliferation compared with the NG group (Fig. 1E; $P<0.05$), but that MMP9 siRNA-transfected podocytes were resistant to this effect.

HG treatment affects the expression of MMP9, α-SMA, podocalyxin and fibronectin-1 in podocytes. The expression levels of MMP9, α-SMA, podocalyxin and fibronectin-1 mRNA and protein in cultured human podocytes were assessed by RT-qPCR and western blotting, respectively. HG treatment significantly increased the expression levels of MMP9, α-SMA and fibronectin-1, and reduced the expression levels podocalyxin compared with NG-treated cells (Fig. 2A-C). These data further supported the hypothesis that HG levels may promote podocyte EMT by altering the expression of MMP9, α-SMA, podocalyxin and fibronectin-1 *in vitro*.

To further characterize the relationship between MMP9 and the expression of α-SMA, podocalyxin and fibronectin-1, MMP9 was down regulated with MMP9-siRNA transfection in cultured human podocytes. MMP9 knockdown significantly reduced the expression levels of α-SMA and fibronectin-1, but increased the expression levels of podocalyxin in both NG and HG-treated human podocytes compared to the respective untransfected groups (Fig. 2A-C). These results suggested
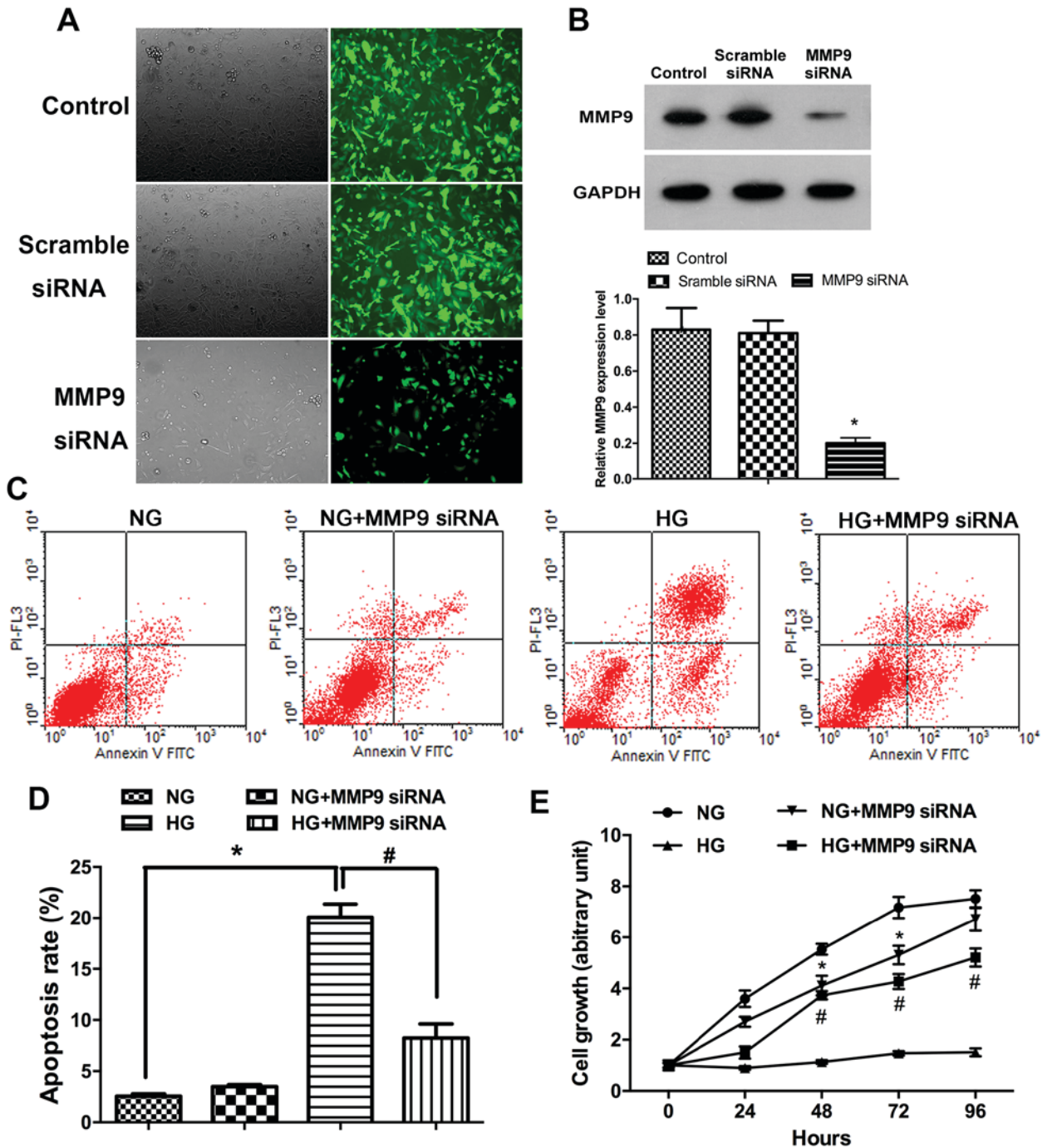
Figure 1. Effects of glucose treatment on apoptosis and proliferation of cultured human podocytes. The expression of MMP9 was evaluated using (A) fluorescence microscopy and (B) western blotting in human podocytes following MMP9-siRNA gene silencing. Experiments were performed in triplicate; *P<0.05 vs. Control. (C and D) Apoptosis was assessed by flow cytometry in human podocytes treated with NG or HG with or without MMP9-siRNA transfection. (E) MTT assays were performed to determine cell proliferation. Experiments were performed in triplicate; *P<0.05 vs. NG; #P<0.05 vs. HG. FITC, fluorescein isothiocyanate; HG, high glucose; MMP9, matrix metalloproteinase 9; NG, normal glucose; PI, propidium iodide; siRNA, small interfering RNA.

that MMP9 may alter the physiological characteristics of podocytes by regulating the expression of α-SMA, podoca-lyxin and fibronectin-1 *in vitro*.

HG treatment induces MMP9 promoter demethylation. To investigate the relationship between MMP9 promoter demeth-ylation and podocyte EMT following HG treatment, the methylation status of 12 CpG sites within the MMP9 promoter region were analyzed (Fig. 3A). In the HG-treated group,

CpG sites 3, 6, 7, 8 and 11 exhibited apparent demethylation compared with NG-treated cells (Fig. 3B), which suggested that HG treatment may be able to induce demethylation of CpG sites in the MMP9 promoter region.

Promoter demethylation upregulates MMP9 expression in vitro. Previously, methylation of promoter region CpG sites was reported to hinder the binding of transcription factors, ultimately inhibiting gene expression (30). To confirm that
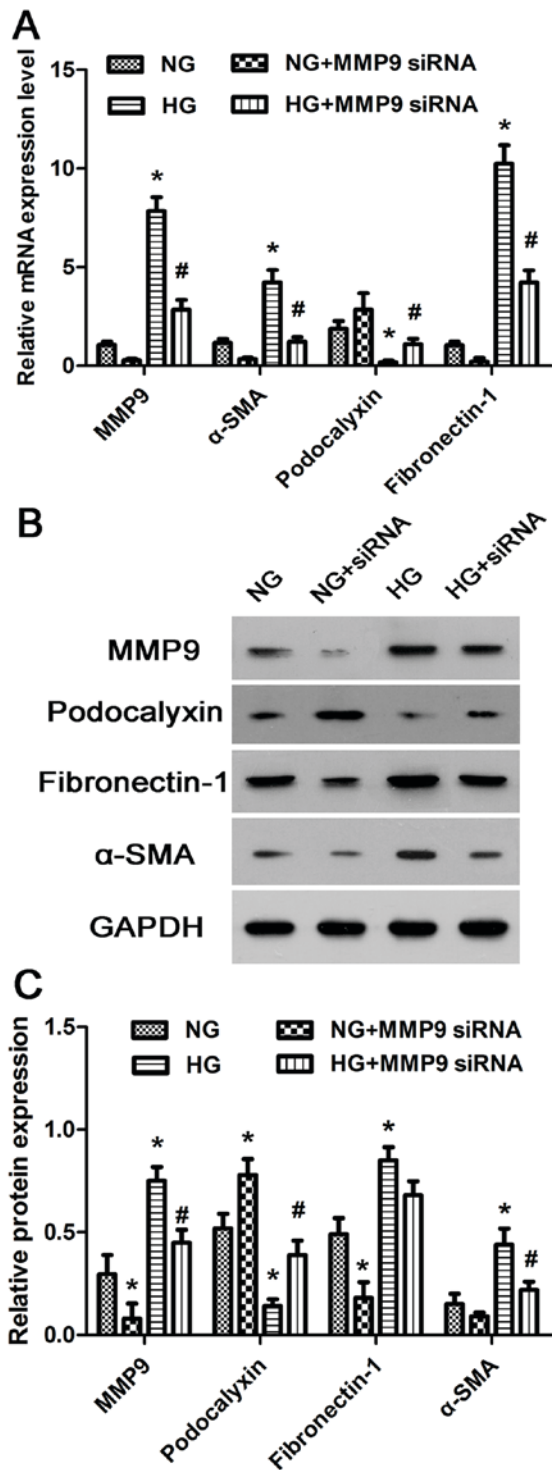
Figure 2. mRNA and protein expression levels of MMP9, α-SMA, podocalyxin and fibronectin-1 in cultured human podocytes treated with HG. (A) Relative mRNA expression levels of MMP9, α-SMA, podocalyxin and fibronectin-1 wereanalyzed in human podocytes by reverse transcription-quantitative polymerase chain reaction. (B) The relative protein expression levels of MMP9, α-SMA, podocalyxin and fibronectin-1 were detected in human podocytes by western blot analysis. (C) Densito metric analysis of protein expression levels from Part B. *P<0.05 vs. NG; #P<0.05 vs. HG. α-SMA, α-smooth muscle actin; HG, high glucose; MMP9, matrix metalloproteinase 9; NG, normal glucose; siRNA, small interfering RNA.

demethylation of the MMP9 promoter region resulted in an up regulation of MMP9 expression, a reporter construct in which the MMP9 promoter specific region was ligated to a

dual luciferase reporter vector was used. The results demonstrated that MMP9 promoter demethylation significantly increased luciferase activity of this reporter, which suggested that the expression of MMP9 was regulated by themethylation status of the MMP9 promoter region (Fig. 3C). Therefore, the present study speculated that methylation of the MMP9 promoter region at the CpG sites may hinder the binding of transcription factors, thus inhibiting expression of MMP9.

DN induces podocyte EMT by regulating expression of MMP9, α-SMA, podocalyxin and fibronectin-1 in vivo. To simulate DN *in vivo*, Wistar rats were in traperitoneally injected with STZ (Fig. 4A). The blood glucose levels significantly increased within the DN group at 2 weeks and 6 weeks compared with in the control. Furthermore, the blood glucose levels significantly increased within the DN group at 6 weeks compared with at 2 weeks (P<0.05; Fig. 4B). There were no marked variations between the control and DN group body weights at 2 weeks, but were significantly decreased in the DN group at 6 weeks compared with in the control group. Furthermore, the body weights significantly increased within the control group at 6 weeks compared with at 2 weeks (P<0.05; Fig. 4C).

To investigate the relationship between MMP9 expression and podocyte EMT *in vivo*, the protein expression levels of MMP9, α-SMA, podocalyxin and fibronectin-1 in the podocytes of DN and control rats were examined. It was revealed that the expression of MMP9, α-SMA and fibronectin-1 was significantly higher and the expression of podocalyxin was significantly lower in DN model rats compared with expression levels in rats in the Control group, as detected by immunohistochemistry and western blotting (Fig. 5A and B, respectively). In addition, the level of demethylation of the MMP9 promoter CpGs was significantly higher in DN rats (Fig. 5C). These *in vivo* data were consistent with the *in vitro* results, and further support the hypothesis that demethylation of the MMP9 promoter may serve an important role in podocyte EMT in DN.

Discussion

DNA methylation involves the addition of a methyl group to DNA, and is an important epigenetic modification. DNA methylation is widespread in the human genome and mainly occurs on the cytosines of CpGdinucleo tides (31). Methylation of gene promoter regions may lead to long-term silencing of gene expression by preventing the binding of transcription factors (32). Aberrant promoter demethylation has been associated with the over expression of genes that are involved in the pathogenesis of many diseases, and thus may potentially be used as disease biomarkers (33,34).

The pre-test of the present study indicated that the expression of MMP9 in podocytes was significantly increased in DN, which led to investigations of the factors affecting MMP9 expression in podocytes incubated with high concentrations of glucose. Previous study also indicated that site-specific demethylation of the MMP9 promoter significantly influenced MMP9 expression in keratinocytes stimulated by tumor necrosis factor α (TNFα) (35,36). In the present study, human podocytes were incubated in media containing high concentrations of glucose. This condition was demonstrated to promote demethylation of the MMP9 promoter and to significantly up regulate MMP9
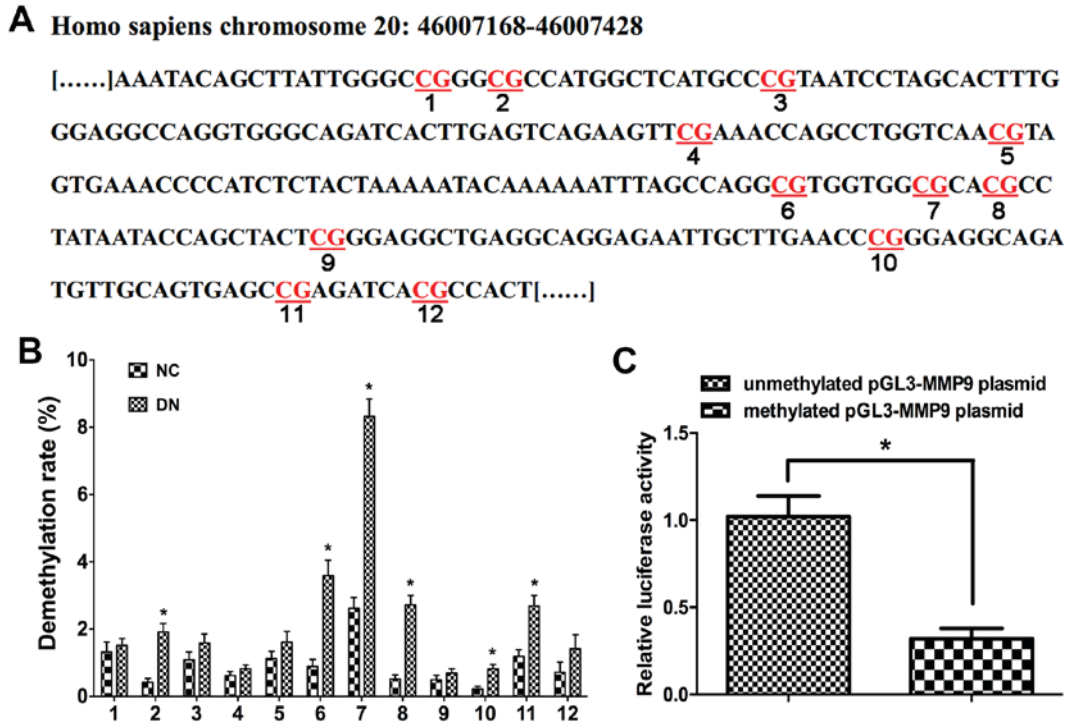
Figure 3. DNA demethylation of specific CpG sites within the human MMP9 promoter region *in vitro*. (A) Identification of 12 CpG sites within the promoter region of human MMP9 gene. (B) MMP9 promoter demethylation levels were assessed by bisulfite sequencing PCR.*P<0.05 vs. NG. (C) *In vitro* methylation of human MMP9 promoter region decreased its promoter activity, as detected by a luciferase reporter assay. Luciferase activity was measured following transfection of 293T cells with the unmethylated or methylated pGL3 Basic MMP9 plasmid. *P<0.05 vs. unmethylated pGL3-MMP9 plasmid. MMP9, matrix metalloproteinase 9.
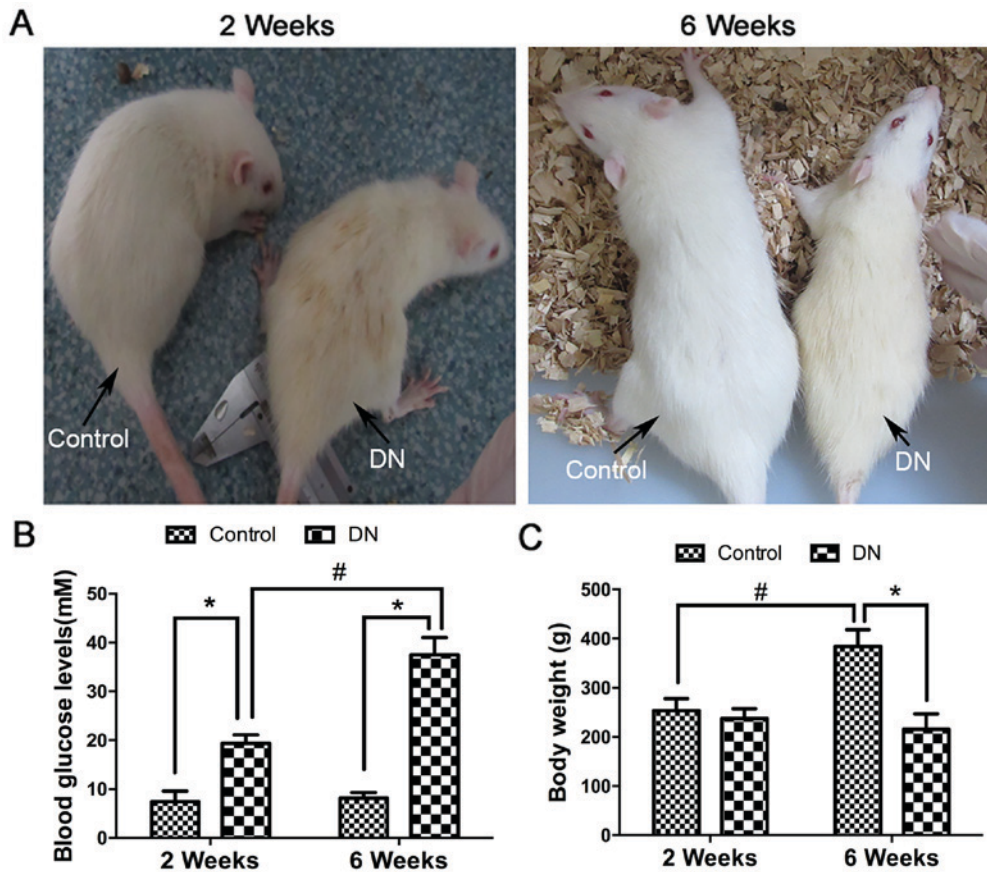

Figure 4. Blood glucose level and body weight of DN rats. (A) DN was induced in rats by STZ. Wistar rats were photographed 2 and 6 weeks following STZ injection. (B) Blood glucose levels of Wistar rats following STZ injection at 2 and 6 weeks. (C) Body weights of Wistar rats following STZ injection at 2 and 6 weeks. *P<0.05 vs. Control, #P<0.05 vs. 2 weeks. DN, diabetic nephropathy; STZ, streptozotocin.
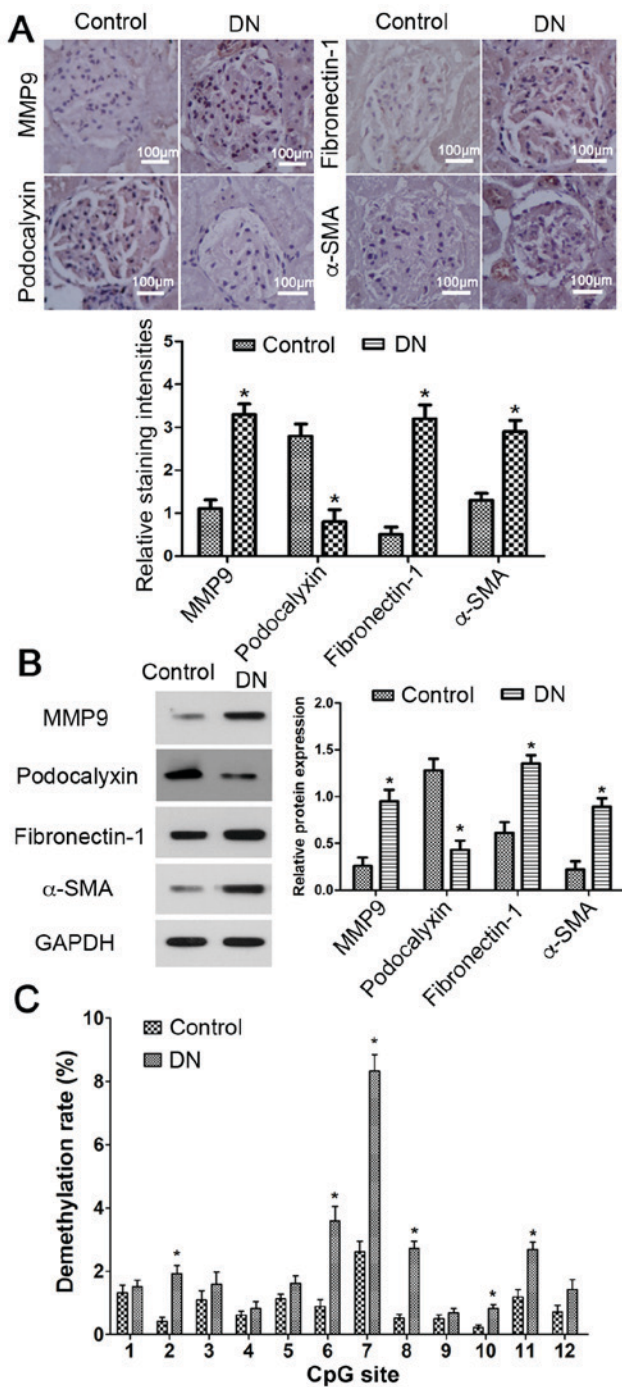
Figure 5. Effects of STZ treatment on expression of MMP9, α-SMA, podocalyxin and fibronectin-1 in DN rats. (A) Expression levels of MMP9, α-SMA, podocalyxin and fibronectin-1 in the podocytes of DN rats were examined dimmunohistochemically. Staining intensity (%), the average positive stained cells percentage to evaluate the slice immunohistochemistry result, measured by Image J software. All the experiments were performed in triplicate. (B) The relative protein expression levels of MMP9, α-SMA, podocalyxin and fibronectin-1 protein in the podocytes of DN rats were examined by western blotting. (C) Demethylation level analysis of MMP9 promoter *in vitro*. *$P<0.05$ vs. Control. α-SMA, α-smooth muscle actin; DN, diabetic nephropathy; MMP9, matrix metalloproteinase 9; STZ, streptozotocin.

expression. Similarly, MMP9 expression was also increased in DN model rats by demethylation of the MMP9 promoter region. The results of the present study revealed that HG levels induced site-specific demethylation of the MMP9 promoter

region, enhancing MMP9 expression. These results suggested that the demethylation status of the MMP9 promoter may be used as a prognostic marker of DN in the clinics.

During EMT, polarity and cell-cell adhesions are lost and the epithelial cells become mesenchymal stem cells, gaining migratory and invasive properties. In addition to normal physiological processes such as neural tube formation, EMT occurs in several pathological events, including cancer, organ fibrosis and chronic inflammation (37,38). EMT was first identified as an important differentiation and morphogenetic process during embryonic development and has been implicated in renal interstitial fibrosis caused by diabetes (39). A number of molecular mechanisms contribute to EMT, including the activation of growth factors and their receptors by proteases, and the cleavage of cellular adhesion molecules (40). MMPs, in particular MMP9, were also previously implicated in EMT (41,42). For example, serum levels of TNF-α were demonstrated to be significantly elevated in patients with renal cell carcinoma (RCC), which induced EMT and promoted tumorigenicity of RCC by repressing E-cadher in, up regulating viment in, activating MMP9 and increasing invasion activities (43).

The present study investigated the association between MMP9 and EMT in podocytes by assessing the degree of MMP9 promoter demethylation that was induced by HG treatment *in vitro* and *in vivo*, and demonstrated that HG treatment may up regulate the expression of MMP9 by inducing demethylation of the MMP9 promoter region. In addition, expression levels of the mesenchymal cell markers α-SMA and fibronectin-1 were increased in HG-treated podocytes, whereas the expression levels of podocalyxin, a marker of podocytes, were significantly reduced. These data suggested that MMP9 promoter demethylation may induce podocyte EMT indirectly. First, expression of MMP9 was associated with the degree of MMP9 promoter demethylation. Second, HG treated podocytes *in vitro* had exhibited an increase in MMP9 promoter demethylation and in the expression levels of MMP9, α-SMA and fibronectin-1, and reduced expression of podocalyxin. Third, dual luciferase reporter assays demonstrated that demethylation of MMP9 promoter significantly influenced its promoter activity. Fourth, a rat model of DN exhibited an increase in the expression levels of MMP9, α-SMA and fibronectin-1, and a decrease in the expression of podocalyxin in podocytes. HG levels induced demethylation of the MMP9 promoter region, enhancing MMP9 expression in podocytes, ultimately promoting podocyte EMT. However, the mechanism that MMP9 promoter demethylation promotes podocyte EMT remains unknown, and will need to be further studied in the future.

In summary, the present results provided preliminary insights into the regulatory roles of MMP9 promoter demethylation and podocyte EMT. These data indicated that MMP9 promoter demethylation may serve an important role in podocyte EMT. Further investigations will be required to determine the precise regulatory mechanisms involved in this process *in vitro* and *in vivo*. The present data may contribute to the future development of novel therapeutic strategies to treat DN.

References

1. Gamella-Pozuelo L, Fuentes-Calvo I, Gomez-Marcos MA, Recio-Rodriguez JI, Agudo-Conde C, Fernandez-Martin JL, Cannata-Andia JB, Lopez-Novoa JM, Garcia-Ortiz L and Martinez-Salgado C: Plasma cardiotrophin-1 as a marker of hypertension and diabetes-induced target organ damage and cardiovascular risk. Medicine (Baltimore) 94: e1218, 2015.
2. Menini S, Iacobini C, Ricci C, Blasetti Fantauzzi C and Pugliese G: Protection from diabetes-induced atherosclerosis and renal disease by D-carnosine-octylester: Effects of early vs late inhibition of advanced glycation end-products in Apoe-null mice. Diabetologia 58: 845-853, 2015.
3. Khan S, Jena G and Tikoo K: Sodium valproate ameliorates diabetes-induced fibrosis and renal damage by the inhibition of histone deacetylases in diabetic rat. Exp Mol Pathol 98: 230-239, 2015.
4. Leehey DJ, Zhang JH, Emanuele NV, Whaley-Connell A, Palevsky PM, Reilly RF, Guarino P, Fried LF and VA NEPHRON-D Study Group: BP and renal outcomes in diabetic kidney disease: The veterans affairs nephropathy in diabetes trial. Clin J Am Soc Nephrol 10: 2159-2169, 2015.
5. Zhao L, Wang X, Sun L, Nie H, Liu X, Chen Z and Guan G: Critical role of serum response factor in podocyte epithelial-mesenchymal transition of diabetic nephropathy. Diab Vasc Dis Res 13: 81-92, 2016.
6. Chen XW, Du XY, Wang YX, Wang JC, Liu WT, Chen WJ, Li HY, Peng FF, Xu ZZ, Niu HX and Long HB: Irbesartan ameliorates diabetic nephropathy by suppressing the RANKL-RANK-NF-κB pathway in type 2 diabetic db/db mice. Mediators Inflamm 2016: 1405924, 2016.
7. Zhang Y, Ma KL, Liu J, Wu Y, Hu ZB, Liu L, Lu J, Zhang XL and Liu BC: Inflammatory stress exacerbates lipid accumulation and podocyte injuries in diabetic nephropathy. Acta Diabetol 52: 1045-1056, 2015.
8. Sweetwyne MT, Gruenwald A, Niranjan T, Nishinakamura R, Strobl LJ and Susztak K: Notch1 and Notch2 in Podocytes Play Differential Roles During Diabetic Nephropathy Development. Diabetes 64: 4099-4111, 2015.
9. Yasuda-Yamahara M, Kume S, Tagawa A, Maegawa H and Uzu T: Emerging role of podocyte autophagy in the progression of diabetic nephropathy. Autophagy 11: 2385-2386, 2015.
10. Andeen NK, Nguyen TQ, Steegh F, Hudkins KL, Najafian B and Alpers CE: The phenotypes of podocytes and parietal epithelial cells may overlap in diabetic nephropathy. Kidney Int 88: 1099-1107, 2015.
11. Zhou HL, Wang YT, Gao T, Wang WG and Wang YS: Distribution and expression of fibroblast-specific protein chemokine CCL21 and chemokine receptor CCR7 in renal allografts. Transplant Proc 45: 538-545, 2013.
12. Omori K, Hattori N, Senoo T, Takayama Y, Masuda T, Nakashima T, Iwamoto H, Fujitaka K, Hamada H and Kohno N: Inhibition of plasminogen activator inhibitor-1 attenuates transforming growth factor-β-dependent epithelial mesenchymal transition and differentiation of fibroblasts to myofibroblasts. PLoS One 11: e0148969, 2016.
13. Brandner JM, Zacheja S, Houdek P, Moll I and Lobmann R: Expression of matrix metalloproteinases, cytokines, and connexins in diabetic and nondiabetic human keratinocytes before and after transplantation into an ex vivo wound-healing model. Diabetes Care 31: 114-120, 2008.
14. Guo J, Xu Y, Ji W, Song L, Dai C and Zhan L: Effects of exposure to benzo[a]pyrene on metastasis of breast cancer are mediated through ROS-ERK-MMP9 axis signaling. Toxicol Lett 234: 201-210, 2015.
15. Zhong Y, Zhang X, Cai X, Wang K, Chen Y and Deng Y: Puerarin attenuated early diabetic kidney injury through down-regulation of matrix metalloproteinase 9 in streptozotocin-induced diabetic rats. PLoS One 9: e85690, 2014.
16. Wang XM, Shi K, Li JJ, Chen TT, Guo YH, Liu YL, Yang YF and Yang S: Effects of angiotensin II intervention on MMP-2, MMP-9, TIMP-1, and collagen expression in rats with pulmonary hypertension. Genet Mol Res 14: 1707-1717, 2015.

17. Lelongt B, Bengatta S, Delauche M, Lund LR, Werb Z and Ronco PM: Matrix metalloproteinase 9 protects mice from anti-glomerular basement membrane nephritis through its fibrinolytic activity. J Exp Med 193: 793-802, 2001.
18. Luo W, Hu L, Li W, Xu G, Xu L, Zhang C and Wang F: Epo inhibits the fibrosis and migration of Müller glial cells induced by TGF-β and high glucose. Graefes Arch Clin Exp Ophthalmol 254: 881-890, 2016.
19. Kang YS, Li Y, Dai C, Kiss LP, Wu C and Liu Y: Inhibition of integrin-linked kinase blocks podocyte epithelial-mesenchymal transition and ameliorates proteinuria. Kidney Int 78: 363-373, 2010.
20. Nakamura T, Ushiyama C, Suzuki S, Hara M, Shimada N, Ebihara I and Koide H: Urinary excretion of podocytes in patients with diabetic nephropathy. Nephrol Dial Transplant 15: 1379-1383, 2000.
21. Thomas MC: Epigenetic mechanisms in diabetic kidney disease. Curr Diab Rep 16: 31, 2016.
22. Ling L, Ren M, Yang C, Lao G, Chen L, Luo H, Feng Z and Yan L: Role of site-specific DNA demethylation in TNFα-induced MMP9 expression in keratinocytes. J Mol Endocrinol 50: 279-90, 2013.
23. Chaturvedi P, Kalani A, Givvimani S, Kamat PK, Familtseva A and Tyagi SC: Differential regulation of DNA methylation versus histone acetylation in cardiomyocytes during HHcy in vitro and in vivo: An epigenetic mechanism. Physiol Genomics 46: 245-255, 2014.
24. Delgado-Olguin P, Dang LT, He D, Thomas S, Chi L, Sukonnik T, Khyzha N, Dobenecker MW, Fish JE and Bruneau BG: Ezh2-mediated repression of a transcriptional pathway upstream of Mmp9 maintains integrity of the developing vasculature. Development 141: 4610-4617, 2014.
25. Jackson MT, Moradi B, Smith MM, Jackson CJ and Little CB: Activation of matrix metalloproteinases 2, 9, and 13 by activated protein C in human osteoarthritic cartilage chondrocytes. Arthritis Rheumatol 66: 1525-1536, 2014.
26. Saleem MA, O'Hare MJ, Reiser J, Coward RJ, Inward CD, Farren T, Xing CY, Ni L, Mathieson PW and Mundel P: A conditionally immortalized human podocyte cell line demonstrating nephrin and podocin expression. J Am Soc Nephrol 13: 630-638, 2002.
27. Livak KJ and Schmittgen TD: Analysis of relative gene expression data using real-time quantitative PCR and the 2(-Delta Delta C(T) method. Methods 25: 402-408, 2001.
28. Baydas G, Nedzvetskii VS, Nerush PA, Kirichenko SV and Yoldas T: Altered expression of NCAM in hippocampus and cortex may underlie memory and learning deficits in rats with streptozotocin-induced diabetes mellitus. Life Sci 73: 1907-1916, 2003.
29. Heiland DH, Ferrarese R, Claus R, Dai F, Masilamani AP, Kling E, Weyerbrock A, Kling T, Nelander S and Carro MS: c-Jun-N-terminal phosphorylation regulates DNMT1 expression and genome wide methylation in gliomas. Oncotarget 8: 6940-6954, 2017.
30. Lewko B, Golos M, Latawiec E, Angielski S and Stepinski J: Regulation of cGMP synthesis in cultured podocytes by vasoactive hormones. J Physiol Pharmacol 57: 599-610, 2006.
31. Pfeifer GP: Mutagenesis at methylated CpG sequences. Curr Top Microbiol Immunol 301: 259-281, 2006.
32. Carr SM, Poppy Roworth A, Chan C and La Thangue NB: Post-translational control of transcription factors: Methylation ranks highly. FEBS J 282: 4450-4465, 2015.
33. Zhang Z, Zhu LL, Jiang HS, Chen H, Chen Y and Dai YT: Demethylation treatment restores erectile function in a rat model of hyperhomocysteinemia. Asian J Androl 18: 763-768, 2016.
34. Lu W, Li J, Ren M, Zeng Y, Zhu P, Lin L, Lin D, Hao S, Gao Q, Liang J, et al: Role of the mevalonate pathway in specific CpG site demethylation on AGEs-induced MMP9 expression and activation in keratinocytes. Mol Cell Endocrinol 411: 121-129, 2015.
35. Zaina S, Goncalves I, Carmona FJ, Gomez A, Heyn H, Mollet IG, Moran S, Varol N and Esteller M: DNA methylation dynamics in human carotid plaques after cerebrovascular events. Arterioscler Thromb Vasc Biol 35: 1835-1842, 2015.
36. Ling L, Ren M, Yang C, Lao G, Chen L, Luo H, Feng Z and Yan L: Role of site-specific DNA demethylation in TNFα-induced MMP9 expression in keratinocytes. J Mol Endocrinol 50: 279-290, 2013.
37. López-Novoa JM and Nieto MA: Inflammation and EMT: An alliance towards organ fibrosis and cancer progression. EMBO Mol Med 1: 303-314, 2009.

38. Cufí S, Vazquez-Martin A, Oliveras-Ferraros C, Martin-Castillo B, Joven J and Menendez JA: Metformin against TGFβ-induced epithelial-to-mesenchymal transition (EMT): from cancer stem cells to aging-associated fibrosis. Cell Cycle 9: 4461-4468, 2010.

39. Zhang W, Miao J, Ma C, Han D and Zhang Y: β-Casomorphin-7 attenuates the development of nephropathy in type I diabetes via inhibition of epithelial-mesenchymal transition of renal tubular epithelial cells. Peptides 36: 186-191, 2012.

40. Song Y, Gong K, Yan H, Hong W, Wang L, Wu Y, Li W, Li W and Cao Z: Sj7170, a unique dual-function peptide with a specific α-chymotrypsin inhibitory activity and a potent tumor-activating effect from scorpion venom. J Biol Chem 289: 11667-11680, 2014.

41. Lee WT, Lee TH, Cheng CH, Chen KC, Chen YC and Lin CW: Antroquinonol from Antrodia Camphorata suppresses breast tumor migration/invasion through inhibiting ERK-AP-1- and AKT-NF-κB-dependent MMP-9 and epithelial-mesenchymal transition expressions. Food Chem Toxicol 78: 33-41, 2015.

42. Lee DG, Lee SH, Kim JS, Park J, Cho YL, Kim KS, Jo DY, Song IC, Kim N, Yun HJ, *et al*: Loss of NDRG2 promotes epithelial-mesenchymal transition of gallbladder carcinoma cells through MMP-19-mediated Slug expression. J Hepatol 63: 1429-1439, 2015.

43. Ho MY, Tang SJ, Chuang MJ, Cha TL, Li JY, Sun GH and Sun KH: TNF-α induces epithelial-mesenchymal transition of renal cell carcinoma cells via a GSK3β-dependent mechanism. Mol Cancer Res 10: 1109-1119, 2012.